Theoretical considerations on the sound power substitution method

Spyros Brezas[1], Martin Schmelzer[2], Volker Wittstock[3]

[1] *Physikalisch Technische Bundesanstalt, 38116 Braunschweig, E-Mail:spyros.brezas@ptb.de*
[2] *Physikalisch Technische Bundesanstalt, 38116 Braunschweig, E-Mail: martin.schmelzer@ptb.de*
[3] *Physikalisch Technische Bundesanstalt, 38116 Braunschweig, E-Mail: volker.wittstock@ptb.de*

Introduction

Sound power is widely used as the descriptor of acoustic emission from sound sources. This is mainly due to its independency of the outer sound field, which is a valid assumption for sufficiently broad frequency bands. The use of the free-field sound power as an alternative descriptor is proposed, in order to extend the validity of the current measurement procedures. This may be achieved by establishing traceability for the free-field sound power, which includes the substitution method [1].

Results of the substitution method based on measurement data have already been presented [2,3]. The present contribution discusses a theoretical study on the factors that influence the substitution method. The basis for the study are numerical calculations including both sound pressure and sound intensity. The effect of reflections was investigated using both the Sommerfeld integral for spherical waves [4] and the mirror source approach for plane waves [5-6]. Under investigation was also the positioning of the source within the measurement surface.

Substitution method

The substitution method is used for the determination of the unknown sound power level of a source S' based on the known sound power level of another source S [1]. It also includes the measurement of a field quantity (sound pressure or sound intensity). The equation, which describes the substitution method is:

$$L_{W,\mathrm{S}'} = L_{W,\mathrm{S}} + \overline{L}_{p,\mathrm{S}'} - \overline{L}_{p,\mathrm{S}} \tag{1}$$

or

$$L_{W,\mathrm{S}'} = L_{W,\mathrm{S}} + \overline{L}_{I,\mathrm{S}'} - \overline{L}_{I,\mathrm{S}} \tag{2}$$

where $L_{W,\mathrm{S}'}$ and $L_{W,\mathrm{S}}$ is the sound power level of the source S' and S respectively. $\overline{L}_{p,\mathrm{S}'}$, $\overline{L}_{p,\mathrm{S}}$, $\overline{L}_{I,\mathrm{S}'}$ and $\overline{L}_{I,\mathrm{S}}$ is the time and surface averaged sound pressure or intensity level of each source as well.

Reflections due to infinite reflecting plane

The substitution method is used in realistic sound environments, where reflections are apparent. To study the effects of reflections, the model of a point source above an infinite reflecting plane was considered. The theoretical foundations of the model were given by Mechel [4]. Well established examples of the use of the mirror source model in room acoustics applications, which include source-receiver pairs, can be found in [5,6]. Figure 1 shows the geometry of a point source S emitting spherical waves over an infinite reflecting plane, the corresponding mirror source S' and a receiver P.

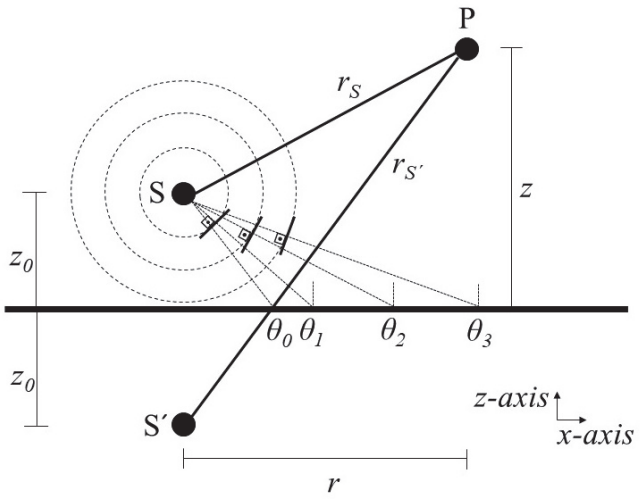

Figure 1: Geometry of the model to investigate the reflections of spherical waves generated by a point source above an infinite reflecting plane.

The sound pressure at the receiver is given by

$$p(x,y,z) = j\rho c k q \frac{e^{-jkr_{\mathrm{S}}}}{4\pi r_{\mathrm{S}}} + p_{\mathrm{refl}} \tag{3}$$

where ρ is the air density, c the sound speed in air, q is the source strength, k the wavenumber and p_{refl} the reflected sound.

As it can be demonstrated by figure 1, the spherical wave of the source S can be decomposed into an infinite number of plane waves, and the reflected wave can be expressed according to [5] as:

$$p_{\mathrm{refl}} = \frac{\rho c k^2 q}{4\pi} \times \int_{\Gamma_\theta} J_0\left(kr\sin\theta\right) e^{-jk\left(z+z_0\right)\cos\theta} R(\theta) \sin\theta \, d\theta \tag{4}$$

where $R(\theta)$ is the complex reflection coefficient of the reflecting plane, which depends on the incidence angle θ and J_0 is the Bessel function of zero order.

In case the incident wave on the reflecting surface is plane eq. 4 becomes:

$$p_{\mathrm{refl}} = j\rho c k q \frac{e^{-jkr_{\mathrm{S}'}}}{4\pi r_{\mathrm{S}'}} R(\theta_0) \tag{5}$$

The sound intensity vector of the source S in the direction of the radial component r_S can be calculated according to [7]:

$$I_r = \frac{1}{2}\mathrm{Re}\left[p(r_S)\cdot u_r^*(r_S)\right] \quad (6)$$

where u_r^* is the complex conjugate of the radial particle velocity, which is given by [7]:

$$u_n(r_S) = -\frac{1}{j\omega\rho}\frac{\partial p(r_S)}{\partial r_S} \quad (7)$$

where ω is the angular velocity.

The measurement of the sound pressure gradient can be approximated and eq. 7 becomes [8]:

$$u_n(r_S) = -\frac{1}{j\omega\rho}\frac{p(r_S+\Delta r/2)-p(r_S-\Delta r/2)}{\Delta r} \quad (8)$$

where Δr is a distance much smaller than the wavelength of interest.

Eq. 8 ensures the calculation of the normal component of the sound intensity, which is required for the sound power determination.

Measurement surface

In room acoustics applications the mirror source model mainly includes a single source-receiver pair. On the contrary, the sound power measurements include average levels over a measurement surface, as indicated by eqs. 1 and 2. The surface can be modelled by a grid of receivers. The distribution of the receivers influences the average level, while the number of the receivers influences the computational time of the calculations.

Figure 2 shows the averaged sound pressure level of a monopole over a hemisphere above a reflecting plane, where only the plane wave approach was used. Two configurations for the distribution of the measurement points were considered. Firstly, the points were placed following a hemispherical path, while in the second the path of a hemispherical helix. In the former case, the sound pressure level at high frequencies alters for different numbers of measurement points, while this is not the case for the latter case. Additionally, computational time may be saved by using a hemispherical helix, since a smaller number of measurement points is required for the same result according to the lower graph of fig. 2. A helicoidal distribution is also more appropriate for the determination of the sound power, because the measurement surface is more representatively sampled.

Spherical wave approach

An important factor that influences the reflection model, is the calculation of the integral of eq. 4, which according to Mechel [4], can be separated into a definite integral for the interval $[0, \pi/2]$ and an improper integral for the interval $[\pi/2+j0, \pi/2+j\infty]$. As it is shown in [5], the improper integral converges except for grazing incidence. Suh [5] calculated the integral of eq. 4 using the Trapezoidal rule stating that the constant step $\Delta\theta$, which replaces $d\theta$, must be as small as possible for accuracy reasons, proposing the value of 10^{-5}.

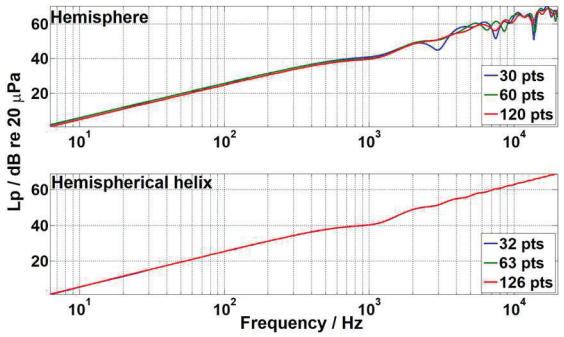

Figure 2: Influence of the measurement points number on the averaged sound pressure level for two different measurement surface configurations.

It must be stated, that the above value does not significantly increase the computational time for the case of a source-receiver pair. In the case of a receiver grid, the value of 10^{-5} becomes extremely detrimental to the calculation time. An investigation was performed to reduce the computational time, without affecting the accuracy of the calculations. For this reason, the averaged sound pressure level and sound intensity level were calculated for both the plane and spherical wave approach. For the latter approach, various values of $\Delta\theta$ were used. Figure 3 shows the difference between the levels according to the plane wave approach and the levels according to the spherical wave approach.

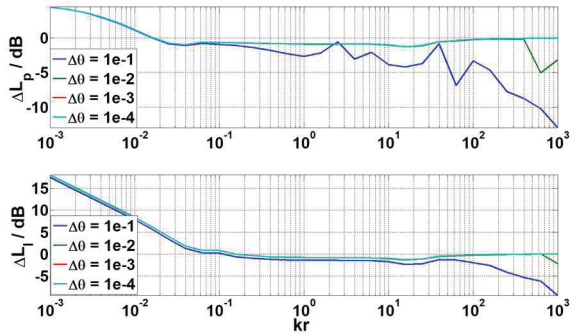

Figure 3: Differences between averaged levels calculated according to plane wave approach and to spherical wave approach for sound pressure (above) and sound intensity (below) for various values of the spherical wave reflection angle discretization step.

For the generalization of the calculations, the distances of interest were expressed as products with the wavenumber. For example, eq. 5 was changed to:

$$p_{\mathrm{refl}} = j\rho c k^2 q\frac{e^{-jkr_{S'}}}{4\pi k r_{S'}}R(\theta_0) \quad (9)$$

As it can be seen in fig. 3, large angle discretization values influence the results. This is not the case for values starting from 10^{-3}. Based on this, the 10^{-3} value was chosen for the further calculations described in the following sections.

Substitution method in free field

An important aspect for the substitution method is the positioning of the source within the measurement grid, along with the relative positioning between the compared sources. For this reason, the sound pressure and sound intensity averaged levels of a monopole were calculated for the case of vertical and horizontal translation compared to the original position. The monopole positions can be seen in fig. 4.

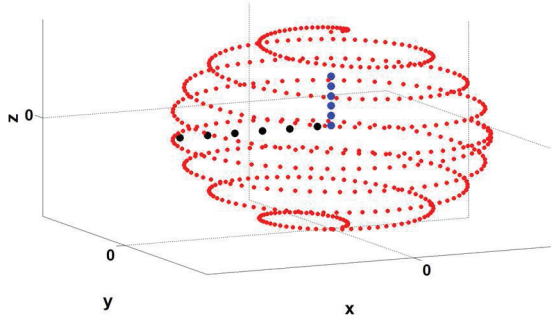

Figure 4: Vertical and horizontal translation of a monopole within a measurement grid.

For the determination of the translation, the position of the monopole was expressed in terms of spherical coordinates ($x = r\sin\theta\cos\varphi$, $y = r\sin\theta\sin\varphi$, $z = r\cos\theta$), where θ is the elevation angle and φ is the azimuthal angle. For the vertical translation, the position of the source was (l_1, 0, 0) and eq. 3 became:

$$p = j\rho c k^2 q \frac{e^{-jkr_S\sqrt{l_1^2/r^2+1-2l_1/r\cos\theta}}}{4\pi k r_S\sqrt{l_1^2/r^2+1-2l_1/r\cos\theta}} \qquad (10)$$

Following the generalization expressed by eq. 9 and by replacing the ratio l_1/r by L_1, eq. 10 was rewritten as:

$$p = j\rho c k^2 q \frac{e^{-jkr_S\sqrt{L_1^2+1-2L_1\cos\theta}}}{4\pi k r_S\sqrt{L_1^2+1-2L_1\cos\theta}} \qquad (11)$$

Similarly, for the horizontal translation the source was located at (l_2, $\pi/2$, π) and the ratio l_2/r was replaced by L_2.

Figure 5 shows the averaged sound pressure and sound intensity level for vertical translation from $L_1 = 0.1$ to $L_1 = 0.5$ and for horizontal translation from $L_2 = 0.1$ to $L_2 = 0.5$. The sound intensity spacer length was set to 4.5 mm. In fig. 5 can be seen that the sound pressure level changes are larger than the sound intensity level changes. The dip in the sound intensity levels at high kr is attributed to the insufficient spacer length.

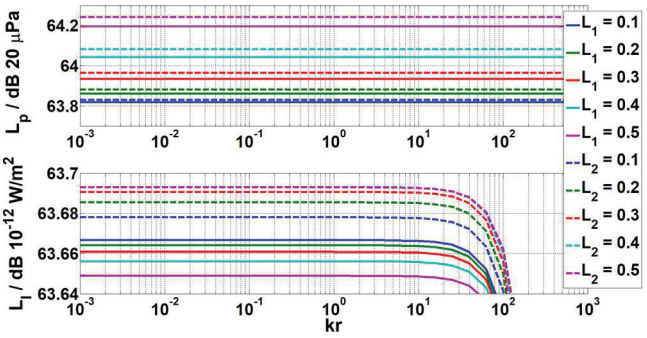

Figure 5: Averaged sound pressure (above) and sound intensity (below) level for a vertically and horizontally translated monopole.

To investigate the influence of the translation to the substitution method, the following procedure was implemented. The substitution was performed for both sound pressure and intensity for vertical and horizontal translation of the unknown source S', which was a monopole. The translations were $L_1 = L_2 = 0.1, 0.2, 0.3, 0.4, 0.5$.

As a known source, a monopole was also used, of the same source strength as the unknown one. The known monopole was positioned at the origin of the axes of the geometry used. The free field sound power of the known monopole is given by [7]:

$$P_{\text{Free}} = \frac{\rho c k^2 q^2}{8\pi} \qquad (12)$$

The sound power level after the substitution method was compared to the free field sound power level in terms of their difference:

$$\Delta L_W = L_{W,\text{Sub}} - L_{W,\text{Free}} \qquad (13)$$

Figure 6 shows the difference (eq. 13) for both vertical and horizontal translation for the case where the substitution method was implemented for sound pressure levels (eq. 1) and for sound intensity levels (eq. 2).

The examination of fig. 6 provides the following findings: the vertical translation of the unknown source yields an overestimation of the free field sound power for the case of sound pressure. The overestimation is larger for the horizontal translation compared to the vertical. For both vertical and horizontal translation, the overestimation increases as the translation also increases. For the case of sound intensity approach, the overestimation is only due to the horizontal translation. On the contrary, the vertical translation yields to underestimation of the free field sound power. The underestimation becomes larger as the translation increases.

Substitution method over reflecting plane

To include the effects of a reflecting plane on the substitution method, the model in fig. 4 was modified by using only the upper part of the measurement grid and placing a highly reflecting plane on its base. The plane wave (eq. 5) and the

spherical wave (eq. 4) approach were taken into consideration and the same analysis as in the previous section was performed.

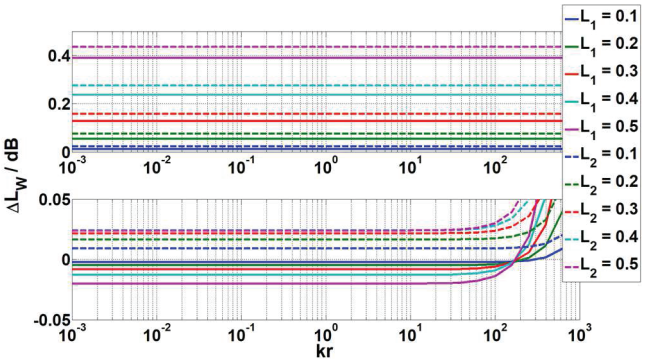

Figure 6: Sound power level difference between substitution method based on sound pressure and sound intensity levels and free field for both vertical and horizontal translation in free field.

Figure 7 shows the sound power level difference according to eq. 13 for the minimum and maximum translation, including both sound pressure and sound intensity as well as both plane and spherical wave approach.

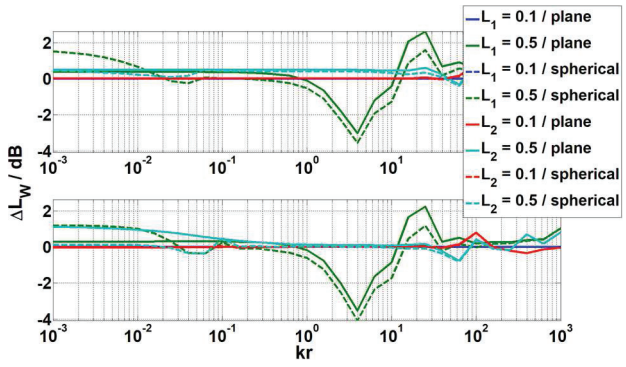

Figure 7: Sound power level difference between substitution method based on sound pressure and sound intensity levels and free field for both vertical and horizontal translation over a highly reflecting plane, for which both plane and spherical wave approach was used.

The reflecting plane influence can be seen in all configurations depicted in fig. 7. The greatest influence is related to the greatest vertical translation. The differences between the plane and the spherical wave approach are apparent for a wide range of kr. The lowest sound power level differences are related to the smallest translations in both the vertical and horizontal plane.

Summary

For the establishment of traceability in sound power, a theoretical study on the substitution method was performed using both sound pressure and sound intensity. A helicoidal distribution of measurement points was suggested. The substitution method was considered in free field conditions and in the case of a highly reflecting plane. For the latter, both plane and spherical wave approach were implemented. For the case of the spherical wave, the discretization of the reflection angle increment was investigated in terms of results and computational time. The influence of the position of the sources within the volume enclosed by the measurement surface was studied. Furtherly, the influence of the sources relative positioning was also studied.

Literature

[1] ISO 3743-1:2010 Acoustics - Determination of sound power levels and sound energy levels of noise sources using sound pressure - Engineering methods for small movable sources in reverberant fields - Part 1: Comparison method for a hard-walled test room

[2] Brezas S., Cellard P., Andersson H., Guglielmone C. & Kirbaş C., Dissemination of the unit watt in airborne sound: aerodynamic reference sound sources as transfer standards, Internoise 2016, Hamburg

[3] Brezas S., Bethke C., Wittstock V., Sound power determination of realistic sources based on the substitution method and sound intensity measurements, DAGA 2017, Kiel

[4] Mechel F. P., Schall-Absorber Band I: Äußere Schallfelder-Wechselwirkungen, S. Hirzel Verlag, 1989

[5] Suh J. S., Nelson P. A., Measurement of transient response of rooms and comparison with geometrical acoustical models, J. Acoust. Soc. Am., 105, 1999

[6] Aretz M., Dietrich P., Vorländer M., Application of the mirror source method for low frequency sound prediction in rectangular rooms, Acta Acust. United Ac., 100, 2014

[7] Fahy F., Walker J., Fundamentals of noise and vibration, Spon Press, 1998

[8] Vér I. L., Beranek L. L., Noise and vibration control engineering, John Wiley & Sons, 2006